

Performance Limits of Cooperative Eigenvalue-Based Spectrum Sensing Under Noise Calibration Uncertainty

Martijn Arts and Rudolf Mathar

Institute for Theoretical Information Technology
RWTH Aachen University, D-52074 Aachen, Germany
Email: {arts, mathar}@ti.rwth-aachen.de

Abstract—A collaborative spectrum sensing system with a fusion center, which utilizes the eigenvalues of the sample covariance matrix for detection, is investigated. On the example of two widely known detectors, we show that imperfect calibration with respect to the noise powers of the receivers leads to a so-called SNR wall in eigenvalue-based detectors. The SNR wall manifests itself as an SNR threshold below which detection becomes impossible even if the number of samples tends to infinity. We quantify the performance limits of the detectors in question by deriving lower bounds on the SNR wall and verify them by numerical evaluation. The results show that a very large number of cooperating receivers is needed to enable detection at very low SNRs, which are customary in spectrum sensing.

Index Terms—eigenvalue-based spectrum sensing, cooperative spectrum sensing, SNR walls, noise uncertainty

I. INTRODUCTION

The scarcity of available spectral resources presents a major challenge for the advance of future wireless communication technologies, where increasing data rates is a key demand. One of the proposed strategies for overcoming this problem is *dynamic spectrum access*, in which unlicensed secondary users (SUs) utilize frequency bands when the licensees, the primary users (PUs), are not using it [1]. An interesting subgroup of research focuses on *opportunistic spectrum access*, where the SUs decide autonomously whether to transmit in vacant frequency bands. Obviously, it is of utmost importance to ensure reliable detection of the presence of PUs, in order to avoid interference for the licensed primary system.

Observing a frequency band in order to decide its occupancy status is known as *spectrum sensing*. Many approaches requiring various degrees of prior knowledge have been investigated [2]. A very widely known approach that requires no knowledge about the PU signal is *energy detection* (ED) [3]. While this detector is very elegant due to its simplicity, its performance is limited severely under uncertainty of the receiver noise power [4]. There exists a so-called *SNR wall*, i.e., an SNR threshold below which detection is impossible even if the number of samples goes towards infinity. More generally, it was shown in [5] that also other detectors proposed in spectrum sensing

This work was partly supported by the Deutsche Forschungsgemeinschaft (DFG) project CoCoSa (grant MA 1184/26-1). This is a revised version of the paper, which corrects some typographic errors. The original uncorrected version can be found in the conference proceedings.

or universally in signal detection [6] suffer from the same phenomenon when uncertainties in the system model exist.

Another class of spectrum sensing detectors that rely on the assumption that receiver noise is uncorrelated is called *eigenvalue-based detection* (EVD). As the name suggests, they evaluate the eigenvalues of the sample covariance matrix for detection. Several different detectors have been proposed, e.g., [2], [7], [8]. Widely known is the maximum-minimum eigenvalue (MME) detector [7] and the generalized likelihood ratio test (GLRT) [8]–[10]. It is commonly claimed that these detectors are immune to the receiver noise uncertainty problem (cf. [7], [8]). The impact of noise estimation techniques for EVD has been studied in [11], [12].

Whether uncertainties in the receiver noise powers may lead to an SNR wall in a cooperative EVD system, however, is still an open problem. In this work, we will answer this question by showing that imperfect calibration will result in an SNR wall. Furthermore, we will quantify the performance limits of two widely known detectors by deriving lower bounds on the SNR wall. For this, a commonly used system model is presented in Section II and the basics of EVD as well as a summary of relevant results about SNR walls in spectrum sensing are given in Sections III and IV, respectively. We introduce a noise calibration uncertainty model in Section V for this investigation. In Section VI we derive lower bounds for the SNR walls of the MME and the GLRT detector and verify the results by numerical evaluation in Section VII.

II. SYSTEM MODEL

We study a spectrum sensing scenario of K cooperating SUs, that strive to determine the occupancy status of a frequency band. Their goal is to determine whether the frequency band in question is currently in use by its PU or not, i.e., to distinguish between two hypotheses based on discrete complex baseband samples. The hypothesis test can be stated as

$$\begin{aligned} \mathcal{H}_0 : \mathbf{y}(t) &= \mathbf{w}(t) \\ \mathcal{H}_1 : \mathbf{y}(t) &= \mathbf{h} s(t) + \mathbf{w}(t). \end{aligned} \quad (1)$$

Under \mathcal{H}_0 , only receiver noise, which is modeled by $\mathbf{w}(t)$, is present. It is assumed that the noise is drawn identically and independently (i.i.d.) for each time-index $t \in \mathbb{N}$ and that it follows a (K -dimensional) zero mean complex circularly sym-

metric Gaussian distribution with a scaled identity matrix $\sigma_w^2 \mathbf{I}$ as its covariance matrix (denoted as $\mathbf{w}(t) \sim \mathcal{CN}(\mathbf{0}, \sigma_w^2 \mathbf{I})$).

Under \mathcal{H}_1 , the PU signal $s(t)$, which is distorted by the communication channel, and additive noise is received. For the sake of simplicity, we assume that the channel is memoryless and the channel coefficients \mathbf{h} remain constant during the sensing interval. The PU signal is simply modeled as a zero mean random variable with variance σ_s^2 of unknown distribution. We assume that the signal and every noise component are independent for each time instance.

The spectrum sensing system employs a cooperative block detection scheme where each SU takes a block of N consecutive samples and sends them to a Fusion Center (FC). A joint decision is taken at the FC by calculating a test statistic on all available samples and subsequently comparing the resulting scalar value to a predetermined threshold γ . It is convenient to use matrix notation to analyze the block detection scheme by combining N consecutive sampled vectors into a $K \times N$ matrix $\mathbf{Y} = [\mathbf{y}(1), \dots, \mathbf{y}(N)]$. This can similarly be done for the noise to gain a noise matrix \mathbf{W} and for the distorted PU signal to attain $\mathbf{X} = \mathbf{h}s$ with the help of the row vector $\mathbf{s} = [s(1), \dots, s(N)]$. Thus, under \mathcal{H}_0 $\mathbf{Y} = \mathbf{W}$ is received, whereas $\mathbf{Y} = \mathbf{X} + \mathbf{W}$ is received under \mathcal{H}_1 . Due to the stationarity of the random processes, the average receiver signal-to-noise ratio (SNR) is constant for the sensing interval and can be defined as

$$\alpha = \frac{\mathbb{E}[\|\mathbf{h}s(t)\|_2^2]}{\mathbb{E}[\|\mathbf{w}(t)\|_2^2]} = \frac{\sigma_s^2 \|\mathbf{h}\|_2^2}{K\sigma_w^2}. \quad (2)$$

This system model is widely used for the analysis of EVD systems, e.g., [10]–[13].

III. EIGENVALUE-BASED DETECTION

A typical assumption in communication systems is that receiver noise is uncorrelated among time and between multiple receivers. In contrast to that, a noisy signal that is oversampled at a single receiver or is simultaneously perceived at multiple receivers shows correlation. This feature is exploited in eigenvalue-based detection by estimating the covariance matrix and calculating a test statistic based on its eigenvalues. The statistical covariance matrix of the received signal is

$$\mathbf{R}_y = \mathbb{E}[\mathbf{y}(t)\mathbf{y}^H(t)] = \begin{cases} \mathbf{R}_0 = \mathbf{R}_w & \text{under } \mathcal{H}_0, \\ \mathbf{R}_1 = \mathbf{R}_x + \mathbf{R}_w & \text{under } \mathcal{H}_1. \end{cases} \quad (3)$$

There, the signal and noise covariance matrices are $\mathbf{R}_w = \sigma_w^2 \mathbf{I}$ and $\mathbf{R}_x = \sigma_s^2 \mathbf{h}\mathbf{h}^H$, respectively.

Let $\boldsymbol{\lambda}$ denote the vector of the ordered eigenvalues of \mathbf{R}_y in ascending order, i.e., $\lambda_1 \leq \lambda_2 \leq \dots \leq \lambda_K$. Then the eigenvalues of the statistical covariance matrix under \mathcal{H}_0 are $\lambda_j = \sigma_w^2$ for $j = 1, \dots, K$. Since \mathbf{R}_x is of rank one and \mathbf{R}_w is a scaled identity matrix, the eigenvalues under \mathcal{H}_1 are readily given by $\lambda_1 = \sigma_s^2 \|\mathbf{h}\|_2^2 + \sigma_w^2$ and $\lambda_j = \sigma_w^2$ for $j = 2, \dots, K$.

In a practical system, the statistical covariance matrix is estimated by the sample covariance matrix, which can be calculated as

$$\hat{\mathbf{R}}_y = \frac{1}{N} \mathbf{Y}\mathbf{Y}^H. \quad (4)$$

Its vector of ordered eigenvalues will be denoted as $\hat{\boldsymbol{\lambda}}$. For $N \rightarrow \infty$, the estimation from (4) converges to the statistical covariance matrix.

In the following, we will introduce two eigenvalue-based detectors that will be utilized in this work.

A. MME

The first work to utilize eigenvalues of the sample covariance matrix for detection in the spectrum sensing context was the maximum-minimum eigenvalue (MME) detector introduced in [7]. As a test statistic the ratio of the largest and the smallest eigenvalue of $\hat{\mathbf{R}}_y$ is used:

$$T_{\text{MME}} = \frac{\max(\hat{\boldsymbol{\lambda}})}{\min(\hat{\boldsymbol{\lambda}})} = \frac{\hat{\lambda}_K}{\hat{\lambda}_1}. \quad (5)$$

B. GLRT

A detector which depends on the ratio of the ratio of the largest eigenvalue and the trace of the sample covariance matrix was reported in [8]. It can also be derived as the generalized likelihood ratio test (GLRT) for the system model from Section II, cf. [9], [10]. We will utilize the detector in an equivalent form in this work, that can be found by realizing that the trace of a matrix can be expressed as the sum of its eigenvalues and utilizing a monotonous nonlinear transformation to gain the test statistic [10]:

$$T_{\text{GLRT}} = \frac{\max(\hat{\boldsymbol{\lambda}})}{\sum_{j=1}^{K-1} \hat{\lambda}_j} = \frac{\lambda_K}{\sum_{j=1}^{K-1} \lambda_j}. \quad (6)$$

IV. SNR WALLS IN SPECTRUM SENSING

To achieve tractable results, performance analysis of detectors is typically performed on simplified models, such as the one from Section II. In a practical application, however, the detector must face the entire complexity of a real world scenario. There, some parameters of the model can never be known exactly. Instead they are only available as estimates up to a finite precision. These uncertainties in the model lead to fundamental limits in detection performance, which cannot be overcome by increasing the sensing time, even if the number of samples tends to infinity. The SNR below which the detector will fail to robustly detect a signal under the model uncertainties in question is called the *SNR wall* [5]. Examples of relevant model uncertainties include the receiver noise (power, spectral coloring, stationarity), the communication channel (fading, stationarity) and receiver imperfections (non-ideal filtering, I/Q imbalance, quantization errors) [6].

To formally define the SNR wall, we closely follow the definition from [6]. Instead of modeling the components of the system with fixed distributions / processes, each component (signal, noise & channel) is allowed to follow any distribution / process belonging to a set, which captures the relevant uncertainties of said component. That is, the PU signal process $s(t)$ may follow any distribution $S \in \mathbb{S}$. This can be analogously defined for the channel process as $H \in \mathbb{H}$ and the noise process $W \in \mathbb{W}$. Let T be any test statistic to be used for block detection operating on N samples with a given

threshold γ , then the probability of false-alarm P_{FA} and the probability of missed detection P_{MD} depending on the tuple (W, S, H) are defined as

$$P_{\text{FA}}(W) = \text{P}(T \geq \gamma \mid \mathcal{H}_0, W), \quad (7)$$

$$P_{\text{MD}}(W, S, H) = \text{P}(T < \gamma \mid \mathcal{H}_1, W, S, H). \quad (8)$$

We say that a detector *robustly* achieves an operating point $(P_{\text{FA}}, P_{\text{MD}})$ if it holds that

$$\sup_{W \in \mathbb{W}} P_{\text{FA}}(W) \leq P_{\text{FA}}, \quad (9)$$

$$\sup_{W \in \mathbb{W}, S \in \mathbb{S}, H \in \mathbb{H}} P_{\text{MD}}(W, S, H) \leq P_{\text{MD}}. \quad (10)$$

A detector is called *non-robust*, if it cannot robustly achieve $(P_{\text{FA}}, P_{\text{MD}})$, with $P_{\text{FA}}, P_{\text{MD}} \in (0, 0.5)$, even if N is arbitrarily large. The SNR wall is then defined as

$$\alpha_{\text{wall}} = \sup\{\alpha_c \mid \text{detector is non-robust } \forall \alpha < \alpha_c\}. \quad (11)$$

Equivalently, the detector is non-robust if the set of medians (or the set of means if the distributions of the test statistic are symmetric) of the test statistic T under both hypotheses overlap.

Most well known is the result about the SNR wall of the energy detector (ED). The ED simply employs the signal energy as test statistic [3]. Thus, the receiver noise power must be known precisely to set the detection threshold. If only an estimation of the noise power is available which lies in the interval $[\rho^{-1}\sigma_w^2, \rho\sigma_w^2]$, then the SNR wall of the energy detector is [4], [5]

$$\alpha_{\text{wall}}^{\text{ED}} = \frac{\rho^2 - 1}{\rho}. \quad (12)$$

Here, the factor $\rho > 1$ describes the amount of uncertainty about the noise power.

Eigenvalue-based detectors relying on the largest eigenvalue for detection, like the MME and the GLRT detector, require a minimum SNR for detection such that the largest eigenvalue under \mathcal{H}_0 and \mathcal{H}_1 can be distinguished [11], [13], i.e., it must hold that

$$\alpha > (\sqrt{KN})^{-1}. \quad (13)$$

Note, however, that this does not lead to an SNR wall, since this threshold is dependent on N .

V. NOISE CALIBRATION UNCERTAINTY IN COOPERATIVE EIGENVALUE-BASED DETECTION

In the literature, eigenvalue-based detectors are commonly thought to be immune to the noise uncertainty problem, see, e.g., [7], [8]. Indeed, if a single SU (exploiting time-correlation) is concerned, the noise power (including the uncertainty factor ρ) may be factored out in both nominator and denominator and thus it cancels out in the ratio for the detectors (5) and (6).

For a cooperative system, knowledge of the noise powers is not needed if and only if the noise powers of the receivers are *exactly* the same. Otherwise, a calibration step must be

performed to scale the noise powers of the receivers to a common level to set the threshold. Assuming this calibration step is perfect is unrealistic and can be refuted by the same reasoning that states a noise power uncertainty must be respected in the first place. Particularly problematic is the fact that the SUs may reside in different geographical locations with diverse environmental characteristics like temperature, humidity and electromagnetic interference that influence the noise powers of the receivers.

In this work, we analyze the influence of a mismatch in noise power calibration of a cooperative eigenvalue-based spectrum sensing system. To investigate this effect in isolation we assume the model from Section II is exact for the channel and the PU signal. The noise is modeled having uncertainty with respect to the noise power calibration of the receivers, such that $W \in \mathbb{W}$, where \mathbb{W} contains all (K -dimensional) zero mean complex circularly symmetric Gaussian distributions with diagonal covariance matrix $\Sigma = \text{diag}(\sigma_{w_1}^2, \dots, \sigma_{w_K}^2)$. There, the noise power of each individual user $j = 1, \dots, K$ may lie in an interval with uncertainty factor ρ , i.e., $\sigma_{w_j}^2 \in [\rho^{-1}\sigma_w^2, \rho\sigma_w^2]$. This models the remaining uncertainty about the noise powers after imperfect calibration and its influence on the detectors will be quantified in the remainder of the paper.

VI. PERFORMANCE LIMITS OF COOPERATIVE EIGENVALUE-BASED DETECTORS

In this section, we investigate the performance limit of the detectors from (5) and (6) under noise calibration uncertainty by deriving lower bounds on the SNR wall. Two scenarios will be analyzed.

First, an average case is studied, where a prior distribution is assigned to the noise uncertainty. For this case, under \mathcal{H}_0 an instance $W \in \mathbb{W}$ will be considered in which the noise powers $\sigma_{w_j}^2$, $j = 1, \dots, K$ are assigned a prior distribution. We assume they are i.i.d. and follow a rectangular distribution with support $[\rho^{-1}\sigma_w^2, \rho\sigma_w^2]$. Under \mathcal{H}_1 , the noise powers are considered to be perfectly calibrated. By showing that the sets of means for the test statistic under both hypotheses overlap in the asymptotic regime ($N \rightarrow \infty$), we prove that there is an SNR wall and obtain a lower bound since the case under investigation does not correspond to the worst case, cf. (11).

Secondly, a worst-case analysis is performed which yields a tighter lower bound on the SNR wall for the MME and the GLRT by investigating the worst case scenario of the test statistic under \mathcal{H}_0 , while again assuming perfect calibration under \mathcal{H}_1 .

Note, that finding the worst-case for imperfectly calibrated receivers under \mathcal{H}_1 leads to the study of complicated non-convex optimization problems.

A. MME

1) *Average case performance limit:* For the lower bound we assume $\sigma_{w_j}^2$, to be i.i.d. and following a rectangular distribution on the support $[\rho^{-1}, \rho]$ for $j = 1, \dots, K$ under \mathcal{H}_0 . Note, that since the noise powers cancel out in the ratio

under both hypotheses for all detectors investigated here, we assume w.l.o.g. $\sigma_w^2 = 1$ for the derivation. The MME test statistic from (5) is the ratio of the extreme eigenvalues. In the asymptotic regime ($N \rightarrow \infty$) these correspond to the largest and the smallest noise powers in the $K \times K$ covariance matrix Σ . Due to the assumptions this is equivalent to studying the order statistic of an affinely transformed standard rectangular distribution with K samples.

Let $U_{(1)} \leq \dots \leq U_{(K)}$ denote the order statistic of a random sample with K samples from a standard rectangular distribution (with support $[0, 1]$) with PDF f_U and CDF F_U . Then the joint PDF of $U_{(1)}$ and $U_{(K)}$ can be found by inserting f_U and F_U into the general form (cf. [14, Th. 5.4.6, p. 230]):

$$f_{(U_{(1)}, U_{(K)})}(u, v) = K(K-1)(v-u)^{(K-2)}, \quad (14)$$

which is valid for $0 \leq u < v \leq 1$ and zero otherwise.

Now the asymptotic mean of the MME test statistic under \mathcal{H}_0 can be found as

$$E_{\mathcal{H}_0}[T_{\text{MME}}] = E \left[\frac{U_{(K)} + (\rho^2 - 1)^{-1}}{U_{(1)} + (\rho^2 - 1)^{-1}} \right], \quad (15)$$

using the affine transformation $(\rho - \rho^{-1})U_{(j)} + \rho^{-1}$ for $j = 1, K$. Let $a := (\rho^2 - 1)^{-1}$. Linearly transforming the joint PDF of $U_{(1)}$ and $U_{(K)}$ from (15) by a in each argument changes only its domain to $a \leq u < v \leq 1+a$. Thus, we can calculate the mean of T_{MME} under \mathcal{H}_0 by solving:

$$\begin{aligned} E \left[\frac{U_{(K)} + a}{U_{(1)} + a} \right] &= \int_{u=a}^{1+a} \int_{v=u}^{1+a} \frac{v}{u} f_{(U_{(1)}, U_{(K)})}(u, v) dv du \\ &= (K-1)(1+a) \int_a^{1+a} \frac{(1+a-u)^{(K-1)}}{u} du + \frac{1}{K}. \end{aligned} \quad (16)$$

The remaining integral in (16) can be found by using the binomial theorem, solving the resulting integrals and rearranging, see (17). Inserting the result into (16), resubstituting a and simplifying we finally gain the desired result as (18).

Unfortunately, (18) is a rather complicated expression which does not seem to possess an easier formulation. As an alternative, we derive an approximation to $E_{\mathcal{H}_0}[T_{\text{MME}}]$ by ignoring the correlation between nominator and denominator and using the marginal distributions. The marginal distribution of the j -th order statistic $U_{(j)}$ is beta distributed, i.e., $U_{(j)} \sim \text{Beta}(j, K-j+1)$ with mean $E[U_{(j)}] = \frac{j}{K+1}$ [14, Ex. 5.4.5, p. 230]. Utilizing a first order bivariate Taylor expansion around the point $(E_{\mathcal{H}_0}[\lambda_K], E_{\mathcal{H}_0}[\lambda_1])$, given as $E_{\mathcal{H}_0}[\frac{\lambda_K}{\lambda_1}] \approx \frac{E_{\mathcal{H}_0}[\lambda_K]}{E_{\mathcal{H}_0}[\lambda_1]}$, it follows that

$$E_{\mathcal{H}_0}[T_{\text{MME}}] \approx \frac{E[(\rho - \rho^{-1})U_{(K)} + \rho^{-1}]}{E[(\rho - \rho^{-1})U_{(1)} + \rho^{-1}]} = \frac{K\rho^2 + 1}{K + \rho}. \quad (19)$$

As already mentioned in Section V, under \mathcal{H}_1 we assume the SUs to be perfectly calibrated, that is $\sigma_{w_j}^2 = \sigma_w^2$ for $j = 1, \dots, K$. Then, assuming $\sigma_w^2 = 1$ again, using the asymptotic eigenvalues from Section III and using (2) we obtain

$$E_{\mathcal{H}_1}[T_{\text{MME}}] = \sigma_s^2 \|\mathbf{h}\|_2^2 + 1 = K\alpha + 1. \quad (20)$$

In order to find the SNR wall, we seek the point at which the mean under both hypotheses overlap, that is the SNR for which $E_{\mathcal{H}_0}[T_{\text{MME}}] \stackrel{!}{=} E_{\mathcal{H}_1}[T_{\text{MME}}]$. Since for this model we have not considered the worst case under both hypotheses, this value will be a lower bound to the actual SNR wall and it holds:

$$\alpha_{\text{wall}}^{\text{MME}} \geq \frac{E_{\mathcal{H}_0}[T_{\text{MME}}] - 1}{K}. \quad (21)$$

By numerically evaluating (18) and inserting the value into (21), a lower bound for the SNR wall under this average case analysis can be investigated. A simple closed-form approximation for this lower bound can be obtained by inserting the approximation from (19) into (21) and simplifying:

$$\alpha_{\text{wall}}^{\text{MME}} \gtrsim \frac{\rho^2 - 1}{K} \left(\frac{K-1}{K + \rho^2} \right). \quad (22)$$

2) *Lower bound on the SNR wall:* In order to obtain a tighter lower bound on the SNR wall we consider a different scenario, where no prior distribution is assigned to the noise power under \mathcal{H}_0 . Instead, a worst-case analysis is performed where it is assumed that $\sigma_{w_j}^2 \in [\rho^{-1}, \rho]$ for $j = 1, \dots, K$. Obviously, for the worst-case under \mathcal{H}_0 , the test statistic is as large as possible. It can be easily seen that this happens when the largest and the smallest eigenvalue attain the largest and smallest possible value in the interval $[\rho^{-1}, \rho]$, respectively. Thus, it holds

$$E_{\mathcal{H}_0}[T_{\text{MME}}] \leq \frac{\rho}{\rho^{-1}} = \rho^2. \quad (23)$$

Inserting (23) into the formula for the SNR wall lower bound from (21), we gain a tighter lower bound on the SNR wall as follows:

$$\alpha_{\text{wall}}^{\text{MME}} \geq \frac{\rho^2 - 1}{K}. \quad (24)$$

Comparing (22) and (24), it is clear that the new bound is always larger than the former bound.

B. GLRT

1) *Average case performance limit:* For the analysis of the average case performance limit of the GLRT detector we make use of the same scenario as introduced in Section VI-A1. As we have seen there, respecting the correlation of the order statistics resulted in a cumbersome expression. Since we expect the same to happen for the GLRT, we directly turn to an approximation for the average case. We will later see in Section VII that this approach is justified.

Analogous to the approximation developed for the MME detector, we ignore the existing correlation between nominator and denominator to derive an approximation to $E_{\mathcal{H}_0}[T_{\text{GLRT}}]$. For the nominator, we can make use of the results from Section VI-A1. The denominator is the sum of the $(K-1)$ remaining eigenvalues, or equivalently put, the sum of all eigenvalues minus the largest one. In principle this can also be related to the order statistic of standard uniformly distributed samples, which was used in Section VI-A1. Since this would involve a rather complex calculation, we approximate the

$$\begin{aligned} \int_a^{1+a} \frac{(1+a-u)^{(K-1)}}{u} du &= \sum_{j=1}^{(K-1)} \binom{(K-1)}{j} (1+a)^{(K-j-1)} \int_a^{1+a} \frac{(-u)^j}{u} du + (1+a)^{(K-1)} \int_a^{1+a} \frac{1}{u} du \\ &= \sum_{j=1}^{(K-1)} \binom{(K-1)}{j} (1+a)^{(K-j-1)} (-1)^j \left(\frac{(1+a)^j}{j} - \frac{a^j}{j} \right) + (1+a)^{(K-1)} \log \left(\frac{1+a}{a} \right) \end{aligned} \quad (17)$$

$$E_{\mathcal{H}_0}[T_{\text{MME}}] = (K-1) \frac{(\rho^{2K})}{(\rho^2-1)^K} \left(\log(\rho^2) + \sum_{j=1}^{(K-1)} \binom{(K-1)}{j} \frac{(-1)^j}{j} (1-\rho^{-2j}) \right) + \frac{1}{K} \quad (18)$$

denominator by the mean of the sum of $(K-1)$ i.i.d. samples from the rectangular distribution with support $[\rho^{-1}, \rho]$:

$$\begin{aligned} E_{\mathcal{H}_0}[T_{\text{GLRT}}] &\approx \frac{E[(\rho - \rho^{-1})U_{(K)} + \rho^{-1}]}{\sum_{j=1}^{(K-1)} E[\sigma_{w_j}^2]} \\ &= 2 \frac{(\rho - \rho^{-1}) \frac{K}{K+1} + \rho^{-1}}{(K-1)(\rho + \rho^{-1})} \end{aligned} \quad (25)$$

$$\approx \frac{(\rho - \rho^{-1}) \frac{K}{K+1} + \rho^{-1}}{(K-1)}. \quad (26)$$

In the last step we used that $E[\sigma_{w_j}^2] = \frac{(\rho + \rho^{-1})}{2} \approx 1$ for the noise uncertainties considered here, say $\rho_{\text{dB}} \leq 2$ dB, where $\rho_{\text{dB}} = 10 \log_{10}(\rho)$.

Under \mathcal{H}_1 , where the receivers are assumed to be perfectly calibrated, the mean of the test statistic can easily be found as

$$E_{\mathcal{H}_1}[T_{\text{GLRT}}] = \frac{K\alpha + 1}{(K-1)}. \quad (27)$$

Finding the SNR for which $E_{\mathcal{H}_0}[T_{\text{GLRT}}]$ and $E_{\mathcal{H}_1}[T_{\text{GLRT}}]$ overlap, results in a lower bound on the SNR wall of the GLRT:

$$\alpha_{\text{wall}}^{\text{GLRT}} \geq \frac{(K-1)E_{\mathcal{H}_0}[T_{\text{GLRT}}] - 1}{K}. \quad (28)$$

Inserting (26) into (28) yields an approximation for the lower bound in this average case scenario:

$$\alpha_{\text{wall}}^{\text{GLRT}} \gtrsim \frac{\rho^2 K + 1}{\rho(K+1)K} - \frac{1}{K}. \quad (29)$$

2) *Lower bound on the SNR wall:* To obtain a tighter lower bound, we again consider the scenario from Section VI-A2, where no prior distribution is assigned to the noise powers of the SUs under \mathcal{H}_0 . It can be seen directly, that the worst case for the GLRT is when the eigenvalues are $\lambda_j = \rho^{-1}$ for $j = 1, \dots, (K-1)$ and $\lambda_K = \rho$, such that

$$E_{\mathcal{H}_0}[T_{\text{GLRT}}] \leq \frac{\rho}{(K-1)\rho^{-1}} = \frac{\rho^2}{(K-1)}. \quad (30)$$

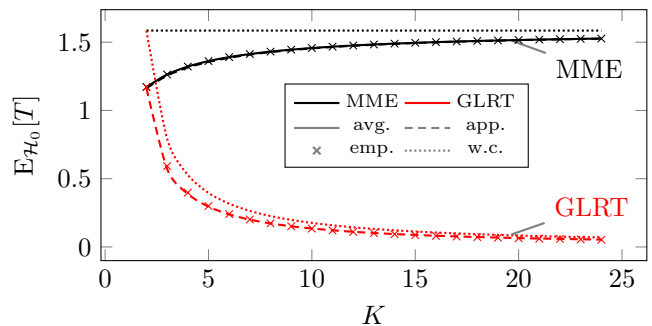
Inserting (30) into (28) finally gives the tighter lower bound

$$\alpha_{\text{wall}}^{\text{GLRT}} \geq \frac{\rho^2 - 1}{K}. \quad (31)$$

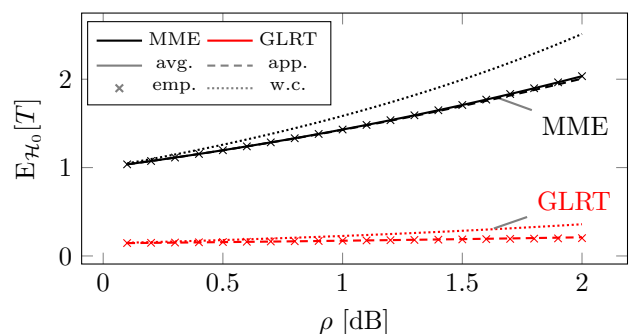
Notice that the tighter lower bound coincides with the one obtained for the MME detector in (24).

VII. NUMERICAL EVALUATION

First, in Figure 1, we inspect the results for the mean of the test statistics under \mathcal{H}_0 that were derived for the MME and the GLRT. The results of a Monte-Carlo simulation with 10^6 trials, where the average case scenario from Sections VI-A1 and VI-B1 was simulated, is used to verify the exact results and the tightness of the approximations. For both the MME and the GLRT we see that the approach chosen for the approximations was justified as the approximation is very tight. At this scale, for small K in Figure 1a a barely noticeable deviance can be observed. For large uncertainties ρ the deviation becomes visible in Figure 1b, but is still negligible for the range of ρ considered here.



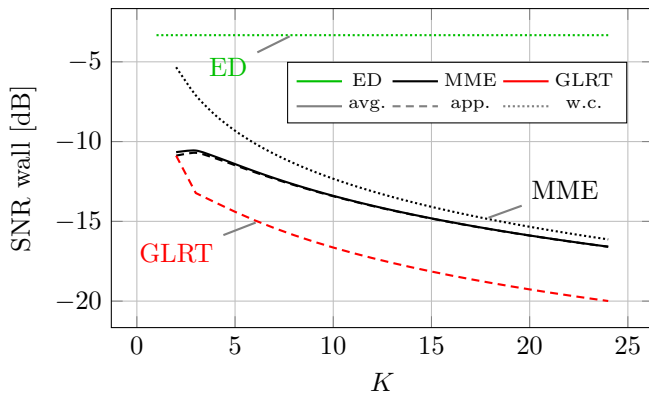
(a) $E_{\mathcal{H}_0}[T]$ for different number of SUs K and $\rho_{\text{dB}} = 1$ dB.



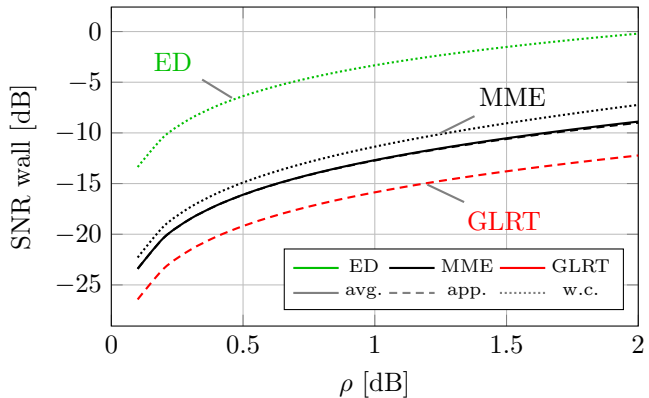
(b) $E_{\mathcal{H}_0}[T]$ for $K = 8$ and different noise uncertainties ρ_{dB} .

Fig. 1. $E_{\mathcal{H}_0}[T]$ for the MME and the GLRT. The plot utilizes the exact formula (avg.) from (18), the approximations (app.) from (19) and (26) and the worst-cases (w.c.) from (23) and (30). Results from a Monte-Carlo simulation (emp.) are drawn to verify the analytical results.

We expect that the GLRT is more robust towards noise uncertainties, since it averages over the noise powers of $K-1$



(a) SNR walls for different number of SUs K and $\rho_{dB} = 1$ dB.



(b) SNR walls for $K = 8$ and different noise uncertainties ρ_{dB} .

Fig. 2. Lower bounds on the SNR wall for the MME and the GLRT. The plot utilizes (21) for the average case (avg.) from (21) using (18), the approximations (app.) from (22) and (29) and the worst-cases (w.c.) from (24) and (31). The SNR wall of the ED from (12) is depicted as a reference.

receivers. Indeed, we see in Figure 1a that as K increases the mean of the MME for the average case scenario converges to the worst-case. This is due to the fact that the MME uses the extreme eigenvalues, which have an increasing likelihood to be near the worst case ones as K increases. Evaluating the relative deviation to the worst-case value for (18) and (26) over K we get a decrease from approximately 26% for $K = 2$ to 3.7% for $K = 24$ for the MME, while the decrease for the GLRT is from 26.6% for $K = 2$ to 21.7% for $K = 24$.

In Figure 2 the lower bounds on the SNR wall of the MME and the GLRT obtained in Section VI are depicted and the SNR wall of the ED is included as a reference. While it seems that the MME and the GLRT improve the value of the SNR wall with respect to the ED, we must keep in mind that we have only obtained lower bounds on the SNR wall. If the SUs are not perfectly calibrated, we must conclude that a very large number of cooperating SUs is needed to be able to detect at the desired SNRs in spectrum sensing ($\alpha \approx -22$ dB). Moreover, while their worst-case lower bound is equal, we see that on average the GLRT is less susceptible to noise calibration uncertainties than the MME.

VIII. CONCLUSION

In this work, we have analyzed the effect of noise calibration uncertainties in a cooperative spectrum sensing system operat-

ing with a fusion center. The investigation was performed on the example of two widely known detectors (MME & GLRT), which operate on the eigenvalues of the sample covariance matrix. A simple system model was utilized, where the signal of one potentially present primary user is observed through a constant memoryless channel with additive white Gaussian noise. To study the fundamental limits of the detectors in question under model uncertainties an imperfect calibration of noise powers of the cooperating secondary users was considered. Two lower bounds for the SNR wall of each detector were derived. The first one with an average case view, where a uniform prior distribution for the noise powers of the receivers was assumed. The second one, in which a worst-case scenario was contemplated. It could be shown that the GLRT is more resilient to noise power calibration uncertainties compared to the MME on average, however, the worst-case lower bounds for the SNR wall of both detectors are equal. More generally, it can be concluded that a very large number of cooperating nodes is needed in the presence of noise calibration uncertainties to successfully detect signals at very low SNRs, which are prevalent in spectrum sensing.

REFERENCES

- [1] Q. Zhao and B. M. Sadler, "A Survey of Dynamic Spectrum Access," *IEEE Signal Processing Magazine*, vol. 24, pp. 79–89, May 2007.
- [2] E. Axell, G. Leus, E. G. Larsson, and H. V. Poor, "Spectrum sensing for cognitive radio: State-of-the-art and recent advances," *IEEE Signal Processing Magazine*, vol. 29, no. 3, pp. 101–116, 2012.
- [3] H. Urkowitz, "Energy detection of unknown deterministic signals," *Proceedings of the IEEE*, vol. 55, pp. 523–531, Apr. 1967.
- [4] A. Sonnenschein and P. Fishman, "Radiometric detection of spread-spectrum signals in noise of uncertain power," *IEEE Transactions on Aerospace and Electronic Systems*, vol. 28, pp. 654–660, July 1992.
- [5] R. Tandra and A. Sahai, "SNR Walls for Feature Detectors," in *2nd IEEE International Symposium on New Frontiers in Dynamic Spectrum Access Networks, 2007. DySPAN 2007*, pp. 559–570, Apr. 2007.
- [6] R. Tandra and A. Sahai, "SNR Walls for Signal Detection," *IEEE Journal of Selected Topics in Signal Processing*, vol. 2, pp. 4–17, Feb. 2008.
- [7] Y. Zeng and Y.-C. Liang, "Maximum-minimum eigenvalue detection for cognitive radio," in *IEEE 18th Annual International Symposium on Personal, Indoor and Mobile Radio Communication*, vol. 7, (Athens, Greece), pp. 1–5, 2007.
- [8] Y. Zeng, Y.-C. Liang, and R. Zhang, "Blindly combined energy detection for spectrum sensing in cognitive radio," *IEEE Signal Processing Letters*, vol. 15, pp. 649–652, 2008.
- [9] P. Bianchi, J. Najim, G. Alfano, and M. Debbah, "Asymptotics of eigen-based collaborative sensing," in *Proceedings of the IEEE Information Theory Workshop (ITW'09)*, 2009.
- [10] A. Taherpour, M. Nasiri-kenari, and S. Gazor, "Multiple antenna spectrum sensing in cognitive radios," *IEEE Transactions on Wireless Communications*, vol. 9, pp. 814–823, Feb. 2010.
- [11] B. Nadler, F. Penna, and R. Garello, "Performance of Eigenvalue-Based Signal Detectors with Known and Unknown Noise Level," in *2011 IEEE International Conference on Communications (ICC)*, pp. 1–5, June 2011.
- [12] P. Dhakal, D. Rivello, F. Penna, and R. Garello, "Impact of noise estimation on energy detection and eigenvalue based spectrum sensing algorithms," in *2014 IEEE International Conference on Communications (ICC)*, pp. 1367–1372, June 2014.
- [13] F. Penna, R. Garello, and M. Spirito, "Probability of Missed Detection in Eigenvalue Ratio Spectrum Sensing," in *IEEE International Conference on Wireless and Mobile Computing, Networking and Communications, 2009. WIMOB 2009*, pp. 117–122, Oct. 2009.
- [14] G. Casella and R. L. Berger, *Statistical inference*, vol. 2. Duxbury Pacific Grove, CA, 2002.